THE JOURNAL OF PHYSICAL CHEMISTRY B

Article

pubs.acs.org/JPCB

# Experimental and Theoretical Approach to Aggregation Behavior of New Di-*N*-Oxide Surfactants in an Aquatic Environment

Agnieszka Lewińska,[†] Maciej Witwicki,[†] Renata Frąckowiak,[‡] Adam Jezierski,[†] and Kazimiera A. Wilk[‡,*]

[†]University of Wrocław, Department of Chemistry, Joliot-Curie14 Str., 50-383 Wrocław, Poland,

[‡]Organic and Pharmaceutical Technology Group, Faculty of Chemistry, Wrocław University of Technology, Wybrzeże Wyspiańskiego 27, 50-370 Wrocław, Poland

**ABSTRACT:** A homologous series of new dicephalic type surfactants (*N*,*N*-bis3,3′-(dimethylamino)propyl]alkylamide di-*N*-oxides) were synthesized and their aggregation phenomena were extensively studied. First, the pH-sensitivity of the investigated surfactants was tested in potentiometric titrations. Then, the adsorption isotherms were measured and interpreted using the Gibbs adsorption equation to determine physicochemical properties. The spin probe EPR technique was employed to monitor the micellization behavior of the surfactants, depending on temperature and surfactant concentration. Critical micelle concentrations (CMC) were determined through an analysis of the calculated spin probe rotational correlation times. A greater insight into the local microenvironment of the formed aggregates was gained by analyzing the properties of the immobilized spin probes. In addition, the CMC values were compared with the ones obtained from tensiometry measurements (taking into account the contributions of the various ionic and nonionic surfactant forms). The approximate size of the micellar aggregates was estimated by the dynamic light scattering (DLS) method. Good agreement between the experimental hydrodynamic radii and those predicted using density functional theory (DFT) guaranteed that the subsequently calculated aggregation numbers, representing the number of molecules in a micelle, were close to the real values. Moreover, the theoretical QSAR methods were used to determine the shape of the micelles via the prediction of the critical packing parameter (CPP).

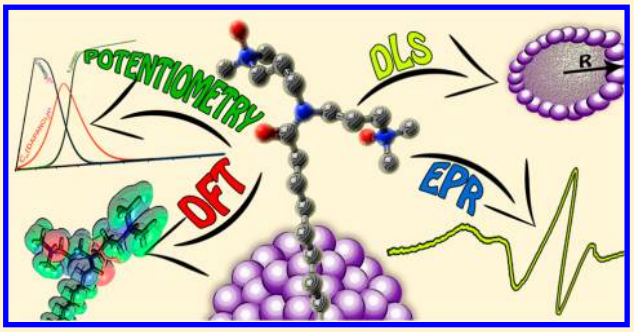


## 1. INTRODUCTION

Recently, there has been a growing interest in designing novel multifunctional surfactants because of modern technological demands to obtain products with specific properties for targeted applications in the area of engineering nanostructures or functional interfaces as well as in the template-assisted fabrication of drug nanocarriers.[1] Surfactants containing more than one headgroup in their structure are known to exhibit a wide range of interesting surface and performance properties making them a multipurpose tool in biological applications. In comparison with single-head/single-chain surfactants, single-chained representatives with multiple head groups have a larger and more hydrophilic end, reducing the activity of the latter significantly and thus manifesting several unique properties in their aggregate states.[1c,2] Among many amphoteric surfactants which are useful for controlling both their aggregation at the interfaces and interactions with biomolecules by simply changing the pH,[3] *N*-oxide-type derivatives constitute an attention-grabbing subclass. Owing to their low toxicity,[3] ready biodegradability,[4] profound surface, and performance properties,[5−9] these single-head structures have made promising surface agents for a variety of pharmaceutical and cosmetic formulations. As mild (or so-called "soft") reagents, *N*-oxide surfactants have been widely applied in various areas of chemistry and biochemistry[6] and that is why their functionalized representatives may constitute promising surface active agents in new nanoscale applications.

As a continuation of our studies on the design and properties of a variety of functionalized surfactants,[1] we present here our contribution dealing with newly synthesized dicephalic *N*,*N*-bis[3,3′-(dimethylamino)propyl]alkylamide di-*N*-oxide ($C_n$(DAPANO)$_2$) surfactants with one hydrophobic tail and two *N*-oxide heads (the structures and abbreviations are shown in Chart 1).

The main purpose of the present contribution was to describe the surface and aggregation behavior of $C_n$(DAPANO)$_2$ derivatives by means of experimental and theoretical methods. Interfacial tensiometry and electron paramagnetic resonance (EPR) spin probe technique[10−12] were used; the latter being an excellent instrument for examining the aggregation behavior of surfactants and their microenvironment characteristics (i.e., microviscosity and local polarity),[10] providing an outstanding supportive basis for surface tension achievements. The 5- and 16-doxylstearic acid (16-DSA and 5-DSA) whose structures are shown in Chart 2) were applied as spin probes for sensing both modifications in

**Received:** June 26, 2012
**Revised:** October 25, 2012
**Published:** October 25, 2012

**Chart 1. Structural Formulas of Dicephalic Di-*N*-oxides $C_n(DAPANO)_2$**

| Structure | R | Abbreviation |
|---|---|---|
| 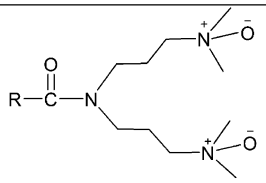 | $C_9H_{19}$ | $C_{10}(DAPANO)_2$ |
| | $C_{11}H_{23}$ | $C_{12}(DAPANO)_2$ |
| | $C_{13}H_{27}$ | $C_{14}(DAPANO)_2$ |
| *N,N-bis[3,3′-(dimethylamino)propyl]alkylamide di-N-oxides* | $C_{15}H_{31}$ | $C_{16}(DAPANO)_2$ |

**Chart 2. Structural Formulas of Spin Probes**

| Structure | Abbreviation |
|---|---|
| 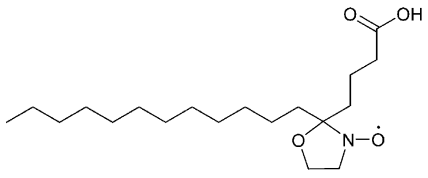 | 5-DSA |
| 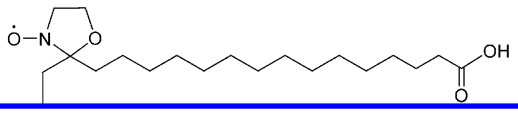 | 16-DSA |

the surfactants' polar head geometry, area as well as local hydration degrees of the hydrophilic moieties, and temperature modifications in the above parameters. Moreover, DLS methods allowed us to estimate the size of micellar aggregates and polydispersity indices. Further analysis of structural properties was performed employing in silico techniques (DFT and QSAR). The structures of the formed aggregates, defined by the critical packing parameter, were predicted with the QSAR approach, while the hydrodynamic radii, micellar volumes, and aggregation numbers were computed with the long-range corrected B3LYP hybrid functional.

The present contribution reports the results of new and original basic research on micellization phenomena of newly synthesized di-*N*-oxide (so-called dicephalic or double-headed) derivatives, treated in both experimental and theoretical manner. The grafting of the amide moiety onto the hydrophobic backbone of the surfactant structure is in agreement with public concerns about the quality of life and provides opportunities to achieve environmentally friendly products with bifunctional capabilities—amenable in the design of surfactant related materials, e.g., template-assisted nanocarriers or biocompatible solubilizing media. The $C_n(DAPANO)_2$ surfactants are attracting particular interest because their synthesis[13] is relatively straightforward and their complex characteristics is important in view of their potential applications.

## 2. MATERIALS AND METHODS

**2.1. Materials.** "{Dicephalic *N,N*-bis[3,3′-(dimethylamino)-propyl]alkylamide di-*N*-oxides ($C_n(DAPANO)_2$) were synthesized (as described in patent[13]) in a two-step reaction of stoichiometric amounts of decanoyl, dodecanoyl, tetradecanoyl and hexadecanoyl chlorides, respectively, with 3,3′-iminobis-(*N,N*-dimethylpropylamine) in a chloroform solution at room temperature in the presence of a saturated $NaHCO_3$ aqueous solution. Crude liquid semiproducts were isolated by means of extraction and purified by conversion to crystalline hydrochlorides in a reaction with gaseous HCl and repeated crystallization from the acetone/chloroform mixture. Then, all of the *N,N*-bis(3,3′-dimethylaminopropyl)alkylamide hydrochlorides were treated with the saturated $NaHCO_3$ aqueous solution to obtain pure *N,N*-bis(3,3′-dimethylaminopropyl)-alkylamides. The last step involved a reaction of the pure semiproducts with hydrogen peroxide (30% solution) in isopropyl alcohol at 50−60°C for 30 h. Then the solvent was evaporated and pure products were obtained. $^1$H NMR (DMSO-$d_6$, 500 MHz) of $C_{12}(DAPANO)_2$ is shown here as an example: 0,90 (t, 3H, $^3J_{HH}$=7,0 Hz, $\boldsymbol{CH_3}(CH_2)_8CH_2CH_2CON$-); 1,28−1,32 (m, 16H, $CH_3(\boldsymbol{CH_2})_8CH_2CH_2CON$-); 1,60−1,65 (m, 2H, $CH_3(CH_2)_8\boldsymbol{CH_2}CH_2CON$-); 2,21−2,30 (m, 4H, -N-$[(CH_2\boldsymbol{CH_2}CH_2N(O)(CH_3)_2]_2$); 2,36 (t, 2H, $^3J_{HH}$=7,5 Hz, $CH_3(CH_2)_8CH_2\boldsymbol{CH_2}CON$-); 3,29 and 3,43 (s, 6H and s, 6H, -N$[(CH_2CH_2CH_2N(O)(\boldsymbol{CH_3})_2]_2$); 3,51 and 3,75 (t, 2H, $^3J_{HH}$=6,6 Hz and t, 2H, $^3J_{HH}$=7,8 Hz, -N$[(CH_2CH_2\boldsymbol{CH_2}N(O)$-$(CH_3)_2]_2$); 3,55−3,60 (m, 4H, -N$[(\boldsymbol{CH_2}CH_2CH_2N(O)$-$(CH_3)_2]_2$). $C_n(DAPANO)_2$ series do not exhibit Krafft points in the temperature range of 277- 373K. The two spin probes (16-doxylstearic acid (16-DSA) and 5-doxylstearic acid (5-DSA), see Chart 2) used in the EPR experiments were purchased from Aldrich Chemical Co. (Milwaukee, WI). The water used in all of the experiments was doubly distilled and purified using the Millipore (Bedford, MA) Milli-Q purification system.

**2.2. Potentiometric Measurements.** Equilibrium constants for the protonation of N-oxide groups were determined by the pH-potentiometric titration of 1.5 cm$^3$ samples of surfactant solutions in HCl ($C$ = 4 mM, $I$ = 0.1 M). The electrode system was calibrated each day by the titration of a HCl solution ($C$ = 4 mM, $I$ = 0.1) against the standard NaOH solution. The resulting titration data were used to calculate the standard electrode potentials. In the calculations, p$K_w$ = 13.77


dx.doi.org/10.1021/jp306282m | J. Phys. Chem. B 2012, 116, 14324−14332

was used as the dissociation constant for water. The monitored pH range for the studied systems was 2.50−11.50. The measurements were performed at 298 ± 0.1 K using a MOLSPIN automatic titration system and fixing the ionic strength with KCl. The titrations were carried out using a combination pH electrode (Mettler Toledo InLabmicro Pro). The surfactant concentration was 0.001 M (the exact concentration determined from the potentiometric titration calculations). The titrations were done in triplicate and the equilibrium constants were calculated using the SUPERQUAD computer program with three titration curves.[14] Thanks to this approach, the relative contributions of the diprotonated, monoprotonated, and deprotonated forms of the surfactants could be determined.

**2.3. Surface Tension Measurements.** Equilibrium surface tension measurements were performed using a Krüss K12 microprocessor tensiometer (Krüss, Hamburg, Germany) equipped with a du Nouy Pt−Ir ring (resolution ±0.01 mN/m). The surface tension data presented in this work were obtained as the arithmetic mean of the values received from two independent runs; the data were reproducible within ±0.2 mN $m^{-1}$. Sets of experiments were taken at intervals until no significant change in the surface tension occurred. All of the surface tension measurements were performed at 295 ± 0.1 K. The absence of a minimum in the isotherm curves near CMC is evidence of the purity of the studied surfactants. The chemical stability of the $C_n$(DAPANO)$_2$ aqueous solutions was proved by $^1$H NMR spectroscopy (solutions in $D_2O$, TSP as a standard). The $^1$H NMR spectra taken at weekly intervals during the month of storage indicated no signals shift relative to the TSP.

**2.4. Electron Paramagnetic Resonance (EPR) Measurements.** The aggregation properties of the micellar and premicellar solutions were studied by EPR using the 16-DSA and 5-DSA nitroxide spin probes. The EPR spectra were recorded by a Bruker Elexsys 500 spectrometer operating at the X-band frequency (~9.7 GHz). A microwave power of 4 mW, a modulation amplitude of 1 G, a sweep width of 100 G, a time constant of 82 ms and a conversion time of 164 ms were adopted. The central field was set to 3410 G. The measurement temperatures were adjusted using a B-VT-2000 temperature controller. During the measurements, the temperature was constant within ±0.1 K. In all of the experiments, the spin probe to surfactant molar ratio was set to 1:400 in order to avoid the broadening of the spectral lines due to spin−spin interactions between the nitroxide radicals incorporated into the investigated surfactant systems.[15] The EPR spectra were analyzed using the WinEPR software package version 1.26b.

**2.5. Dynamic Light Scattering (DLS).** The average size (i.e., the hydrodynamic diameter) and polydispersity of the droplets were determined by the DLS method. The measurements were performed using a Nano Series Zetasizer from Malvern Instruments (UK) with a detection angle of 173°, equipped with an He−Ne laser (632.8 nm) and an ALV 5000 multibit multitau autocorrelator. Before the measurements, the samples were filtered through a filter (with a pore size of 0.2 μm) directly into the optical cell to remove any impurities. All of the DLS measurements were performed at 298 ±0.1 K and at a surfactant concentration a hundred times higher than the critical micelle concentration (CMC). Each value was obtained as the average of three runs with at least 10 measurements. The DTS (Nano) program was used to evaluate the data.

**2.6. Density Functional Theory (DFT) Computations.** Density functional theory was employed to calculate the aggregation numbers ($N_{agg}$) for the investigated micellar systems. All of the calculations were carried out using the Gaussian 09 program.[16] The CAM-B3LYP hybrid functional[17] with improved long-range properties was used together with the 6-31++G (d,p) basis set.[18] The solvent (water) effects were taken into account through the integral equation formalism variant of the Tomasi PCM method (IEF-PCM).[19] The optimized geometries of the monomeric surfactants were confirmed to be the true minima by a vibrational analysis. The molecular volumes of the hydrated monomers ($V_{mon}^{DFT}$) were computed using numerical Monte Carlo integration with a density contour of 0.001 e/Bohr$^3$ and an accuracy of 200 points per Bohr.$^3$ In order to reduce the random errors of Monte Carlo integration, $V_{mon}^{DFT}$ was calculated 100 times for each monomeric surfactant and the mean values were used to calculate the aggregation numbers. The micellar radii ($R_H^{DFT}$) were assumed as the distance between the carbon atom of the terminal methyl group and the farthest nitrogen atom of the *N*-oxide group. $N_{agg}$ values were calculated from $R_H^{DFT}$ and $V_{mon}^{DFT}$, assuming a spherical shape of the micellar aggregates. The high accuracy of this procedure[20a] and of DFT techniques[20b−d] had been demonstrated before.

**2.7. Quantitative Structure−Activity Relationship (QSAR).** Another in silico analysis of the surfactants' aggregation properties was performed using QSAR modeling,[21,22] which is a standard computational tool for relating the potential activity (e.g., toxicity or hydrophobicity) of a compound to its structural, physicochemical, or conformational properties represented by multiple chemical descriptors.[22] Calculations of (a) the degree of hydrophobicity, defined as the logarithm of the compound octanol−water partition coefficient (log *P*), and (b) the critical packing parameter (CPP), which defines the type of micelle structure in the solution, were carried out using the algorithm implemented in the HyperChem 8.0 program[23] with the atomic parameters proposed by Viswanadhan et al.[24a] All of the QSAR computations were done for the molecular structures previously optimized using DFT as described above. Log *P* was computed according to method proposed by Ghose et al.[24b] An important advantage of this approach is the evaluation of hydrophobicity on an individual atom basis allowing to avoid any correction coefficients. The factors used to classify atoms into types are for instance: valence geometry (hybridization) of the atom, formal charge density on the atom or approachability of the solvent molecule toward the atom for the undeniable intramolecular interactions.[24b] Therefore, the formula for estimating the octanol−water partition coefficient can be given as follows:

$$\log P = \Sigma n_i a_i$$

where $n_i$ is the number of atoms of type *i*, and $a_i$ is the contribution of the corresponding atom type. CPP was calculated from the following equation:

$$\mathrm{CPP} = V\cdot(a_o\cdot L_c)^{-1} \quad (1)$$

where *V* is the volume of a surfactant monomer, $a_o$ is the optimum (corresponding to the minimum energy) headgroup area and $L_c$ is the maximum possible extension of the flexible hydrophobic chain. The *V* and $a_o$ values were obtained directly from the QSAR computations, $L_c$ was determined (as the distance between the first and the last carbon atom of a hydrophobic chain) from the optimized structures.


dx.doi.org/10.1021/jp306282m | J. Phys. Chem. B 2012, 116, 14324−14332

## 3. RESULTS AND DISCUSSION

**3.1. pH Effect.** In the case of $C_n(DAPANO)_2$, none, one or both of the *N*-oxide head groups can be protonated, and in consequence the studied surfactants can adopt a cationic or neutral form. Hence, the aggregation properties and practical applications of the studied surfactants are strongly dependent on their protonation degree determined by the pH.

The contributions of the differently protonated forms, varying with the pH, were studied here by potentiometric titrations. An equilibrium between the three (di-, monoprotonated and deprotonated) forms present in the water solution was observed. This is shown (together with the obtained p$K_a$ values) in Figure 1. In the case of the pH close to physiological

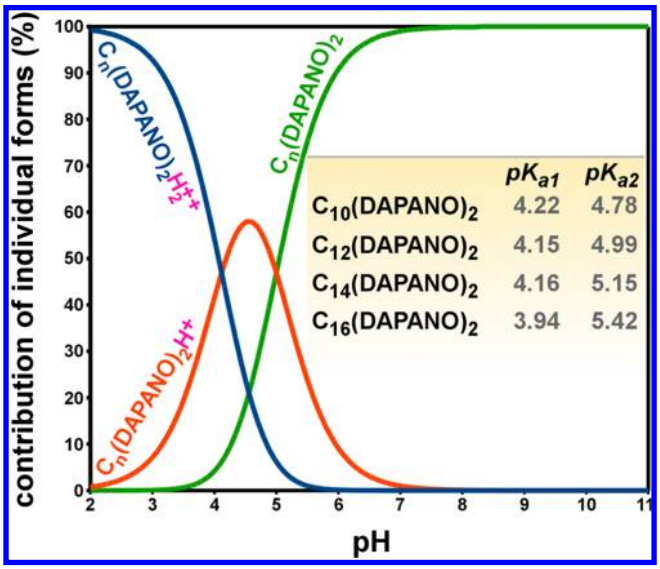


**Figure 1.** Changes in the contribution of deprotonated ($C_n(DAPANO)_2$), mono-($C_n(DAPANO)_2H^+$) and diprotonated ($C_n(DAPANO)_2H_2^{+2}$) forms with pH variation and p$K_a$ values obtained for the acids conjugated with nonionic surfactants (bases).

(~7), the contribution of the monoprotonated form for all of the surfactants was found to be below 3%, hence only the nonionic form is practically adsorbed at the interface and predominately aggregates into micellar systems. In other words, the surfactants of the $C_n(DAPANO)_2$ series can be treated as nonionic at a pH of ~7 or higher. Nevertheless, their pH-sensitivity is a feature worth emphasizing.

**3.2. Adsorption at Air/Solution Interface.** The interfacial behavior of the synthesized $C_n(DAPANO)_2$ was studied through surface tension measurements performed in a wide range of surfactant concentrations. The surface tension isotherms and the adsorption parameters derived from the surface tension data were calculated taking into account the contributions of the various forms, even though they proved to be inconsequential. However, for the sake of the coherence of the discussion it was decided to calculate the isotherms and the adsorption parameters taking the small contributions into account since in the EPR and DLS experiments they are included a priori.

The equilibrium surface tension isotherms for the aqueous solutions of $C_n(DAPANO)_2$ are presented in Figure 2A showing the classical behavior of surface tension with increasing surfactant concentration. As the surfactant concentration is increased, the surface tension decreases to a minimum and does

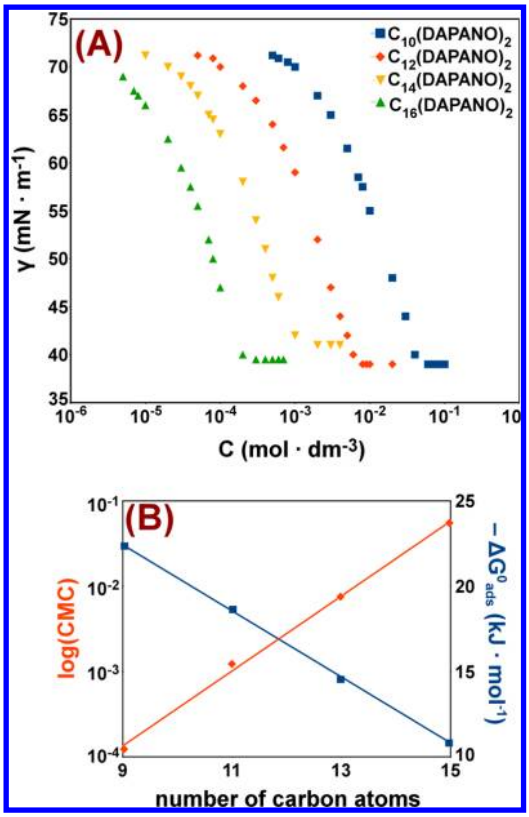


**Figure 2.** (A) Equilibrium surface tension ($\gamma$) of $C_n(DAPANO)_2$ as a function of surfactant concentration; and (B) logarithm of critical micelle concentration (log(CMC), orange line) and standard free energy of adsorption ($\Delta G^0_{ads}$, blue line) of $C_n(DAPANO)_2$ as a functions of the number of carbon atoms in the alkyl chain.

not change as more surfactant is added, whereby the critical micelle concentration can be determined (Figure 2A). Surface activity, measured as $\Delta G^0_{ads}$, increases with alkyl chain length (Figure 2B).

The obtained surface tension data were used to calculate the characteristic adsorption parameters from the Gibbs adsorption equation:

$$\Gamma_\infty = -\frac{1}{nRT}\frac{d\gamma}{d\ln c} \quad (2)$$

where $\Gamma$ [mol/m$^2$] is the surfactant surface excess concentration, $\gamma$ [mN/m] is the surface tension, $c$ [M] is the surfactant concentration, $R$ [J/(mol K)] is the gas constant, and $T$ [K] is the absolute temperature. The numerical (Gibbs) factor $n$ assumes a value of 1 for nonionic surfactants, while for ionic surfactants (with no added electrolyte) its value is determined by the condition of electroneutrality of the adsorbed layer. The minimum surface area demand per molecule, $A_{min}$, was calculated from the equation:

$$A_{min} = \frac{1}{N_A\Gamma_\infty} \quad (3)$$

where $N_A$ is the Avogadro number. The values of the obtained parameters for the investigated surfactants and for other known *N*-oxide representatives are collected in Table 1.

Surface areas occupied by the surfactant at the interface are larger for the investigated herein di-*N*-oxides than for their linear counterparts PDA-n(O) and other dicephalics (4c, 4d, 4e) previously studied by Piasecki et al.[25] Moreover, with


dx.doi.org/10.1021/jp306282m | J. Phys. Chem. B 2012, 116, 14324−14332

**Table 1. Adsorption Parameters of the *N*-Oxide Surfactants**

| compound | surface tension | | | | | | EPR |
|---|---|---|---|---|---|---|---|
| | $\gamma_{CMC}$ (mN/m) | $10^6\ \Gamma_\infty$ (mol/m$^2$) | $10^{20}\ A_{min}$ (m$^2$) | $pC_{20}$ (M) | $-\Delta G^0_{ads}$ (kJ/mol) | CMC (M) | CMC (M) |
| $C_{10}(DAPANO)_2$ | 39.0 | 2.8 | 59.1 | 1.82 | 10.41 | $3.0 \times 10^{-2}$ | $3.3 \times 10^{-2}$ |
| $C_{12}(DAPANO)_2$ | 39.0 | 2.8 | 59.9 | 2.70 | 15.40 | $5.5 \times 10^{-3}$ | $5.7 \times 10^{-3}$ |
| $C_{14}(DAPANO)_2$ | 41.0 | 2.8 | 60.2 | 3.40 | 19.39 | $8.0 \times 10^{-4}$ | $8.1 \times 10^{-4}$ |
| $C_{16}(DAPANO)_2$ | 39.5 | 3.1 | 54.1 | 4.15 | 23.71 | $1.5 \times 10^{-4}$ | $1.5 \times 10^{-4}$ |
| PDA-12(O)[a] | | 3.9 | 42.0 | | 24.8 | $8.0 \times 10^{-4}$ | |
| PDA-14(O)[a] | | 4.1 | 40.5 | | 31.1 | $1.0 \times 10^{-4}$ | |
| 4c[b] | 45.5 | 3.6 | 47 | 3.30 | 18.84 | $1.3 \times 10^{-3}$ | |
| 4d[b] | 48.4 | 3.5 | 47 | 4.10 | 23.38 | $1.5 \times 10^{-4}$ | |
| 4e[b] | 48.0 | 3.2 | 52 | 4.98 | 28.42 | $1.6 \times 10^{-5}$ | |

[a]Data from ref 25a. [b]Data from ref 25b.

**Table 2. Correlation Times ($\tau_R$) and Polarity Indexes ($H$(25° C)) Obtained from the EPR Spectra of 16-DSA in Water Solutions of the $C_n(DAPANO)_2$ Surfactants**

| C/CMC | $C_{10}(DAPANO)_2$ | | $C_{12}(DAPANO)_2$ | | $C_{14}(DAPANO)_2$ | | $C_{16}(DAPANO)_2$ | |
|---|---|---|---|---|---|---|---|---|
| | $\tau_R[10^{-10}]$ | $H$(25° C) | $\tau_R[10^{-10}]$ | $H$(25° C) | $\tau_R[10^{-10}]$ | $H$(25° C) | $\tau_R[10^{-10}]$ | $H$(25° C) |
| 100 | 8.02 | 0.58 | 9.64 | 0.56 | 9.35 | 0.55 | 7.83 | 0.52 |
| 50 | 8.16 | 0.59 | 7.98 | 0.56 | 9.43 | 0.55 | 7.40 | 0.52 |
| 10 | 7.56 | 0.60 | 7.63 | 0.59 | 8.75 | 0.55 | 6.89 | 0.51 |
| 5 | 7.14 | 0.74 | 7.00 | 0.59 | 8.50 | 0.55 | 6.97 | 0.51 |
| 2.5 | 6.66 | 0.94 | 6.89 | 0.91 | 8.50 | 0.84 | 6.06 | 0.87 |
| 1 | 6.77 | 0.98 | 7.01 | 0.91 | 8.50 | 0.84 | 6.06 | 0.87 |
| 0.9 | 1.11 | 1.03 | 1.07 | 1.01 | 1.45 | 0.99 | 0.94 | 0.99 |
| 0.3 | 1.04 | 1.00 | 1.29 | 1.00 | 1.39 | 0.99 | 0.85 | 0.99 |

increasing surfactant alkyl chain length, no change in the minimum surface area required per adsorbed molecule was observed for the examined molecules. Hence, limiting surfactant surface concentration $\Gamma_\infty$, which is directly related to $A_{min}$, remains at the same level for all of the studied di-*N*-oxides. The values of $\Delta G^0_{ads}$ were calculated using the relation introduced by Rosen:[26]

$$\Delta G^0_{ads} = -2.303RT\,pC_{20} \tag{4}$$

where $pC_{20}$ is surface adsorption efficiency as the negative logarithm of bulk surfactant concentration $C_{20}$ required to reduce the surface tension of water by 20 mN/m. The more negative the $\Delta G^0_{ads}$ values, the greater the tendency for the surfactant to adsorb at the air/water interface. Thus, the values of $\Delta G^0_{ads}$ collected in Table 1 show that the linear *N*-oxide surfactants (PDA-n(O)) are more surface active than the respective dicephalics. The dependence of $\Delta G^0_{ads}$ on the number of carbon atoms in the alkyl chain for $C_n(DAPANO)_2$ appears to be linear ($R^2$ = 0.998, see Figure 2B):

$$\Delta G^0_{ads} = -0.45n_C + 5.17 \tag{5}$$

Within any homologous surfactant series, CMC decreases regularly with increasing hydrocarbon chain length and with increasing surface activity of the surfactant. This is a consequence of Traube's rule, which states that within a homologous series of surfactants, each additional methylene group reduces 3-fold the molar concentration required to produce a corresponding reduction in water surface tension. The CMC is reduced by a factor of −log (1/3) = 2 with addition of a methylene group.[26]

**3.3. EPR Studies of Micelle Formation in Water.** The EPR spectra of the investigated systems revealed hyperfine splittings characteristic of nitroxide radicals.[27] For each of the spectra, the rotational correlation time ($\tau_R$) was calculated according to the following:[10b,28,29]

$$\tau_R = (6.51 \times 10^{-10})\cdot\Delta H_{(0)}\cdot\left\{\sqrt{\frac{h_{(0)}}{h_{(-1)}}} + \sqrt{\frac{h_{(0)}}{h_{(+1)}}} - 2\right\} \tag{6}$$

where $h_{(+1)}$, $h_{(0)}$, and $h_{(-1)}$ are the intensities of respectively the low, central, and high field peak of the EPR spectrum, and $\Delta H_{(0)}$ is the width of the central line (in Gauss). Equation 6 is applicable[30] only in the fast motion region, i.e., for $\tau_R$ in the range of $10^{-11} < \tau_R < 3 \times 10^{-9}$ s. By monitoring $\tau_R$ values for 16-DSA the micelle formation was detected and the critical micelle concentration (CMC) determined. The low values of $\tau_R$ (see Table 2) proved that the spin probe was close to full rotation, indicating that micelles did not occur in the water solution and only the monomeric surfactants and the spin probes were located at the water/air interface. In contrast, when the surfactant concentration is equal to or higher than C/CMC, the micelles are formed and the spin probe becomes immobilized, which leads to a significant increase in $\tau_R$. The correlation times derived from the EPR experiments with the use of 16-DSA for the $C_n(DAPANO)_2$ series are listed in Table 2 and have been plotted against the negative logarithm of the surfactant molar concentration to obtain CMC (see Figure 3). The values of CMC are slightly higher than those obtained by tensiometry, which can be explained by the fact that in the EPR experiment an increase in $\tau_R$ is observed only after the micelles have completely formed. The 5-DSA spin probe was found to be unsuitable for determining CMC through EPR measurements due to the short spin relaxation times occurring when the probe is not immobilized. Nevertheless, the probe was found to be valuable in the EPR investigations into the dynamics of the micelles owing to the fact that its radical center


dx.doi.org/10.1021/jp306282m | J. Phys. Chem. B 2012, 116, 14324−14332

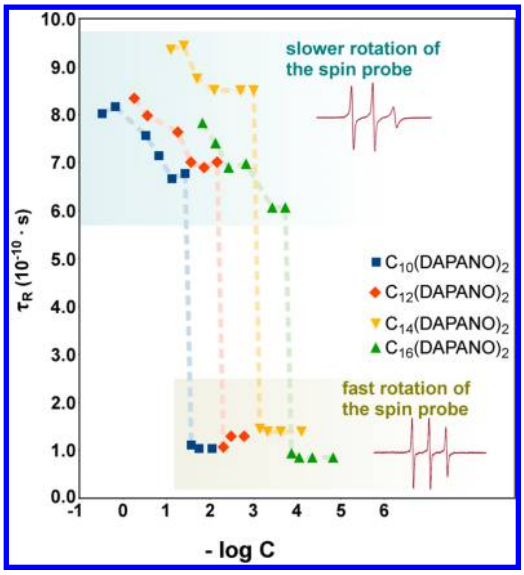


**Figure 3.** Variation of the rotational correlation time ($\tau_R$) of 16-DSA with the $C_n(DAPANO)_2$ concentration, in addition the exemplary EPR spectra are shown.

was located close to the Stern layer of the studied micellar systems. In contrast, the 16-DSA probe was incorporated into the palisade part and therefore was less prone to temperature-induced changes in the dynamics of the aggregates.

**3.4. Temperature Impact on Dynamics and Microenvironment of Micellar Systems.** For the micellar solutions of the $C_n(DAPANO)_2$ series, the correlation times $\tau_R$ derived from the EPR spectra (see Figure 4) decrease with rising temperature for both the spin probes. As temperature rises, the hydrophobic interactions among the surfactant monomers become less significant. In consequence, the distances between the monomeric units lengthen, whereby the micelles grow in size and spin probe immobilization decreases. The values of $\tau_R$ are always higher for 5-DSA incorporated in the hydrophilic part of the micelles than for 16-DSA (Table 3), suggesting stronger immobilization of the former spin probe regardless of temperature. The isotropic hyperfine splitting constant ($a_N$), which describes the interaction between an unpaired electron and the magnetic nucleus, depends on the polarity of the probe environment and can be used to describe local changes in composition around the probe.[31] As the environment polarity increases, spin density in the -N−O• group shifts toward the nitrogen atom,[32] resulting in higher values of $a_N$. Thus, the $a_N$ values can be used to characterize micropolarity, as the latter was shown to vary linearly with nonempirical polarity index $H(T)$ as follows:[33,34]

$$a_N = 14.210 + 1.552H(T) \quad (7a)$$

$$a_N = 14.309 + 1.418H(T) \quad (7b)$$

for 5-DSA and 16-DSA, respectively.

**Table 3. Microenvironment Characteristics of $C_{12}(DAPANO)_2$ Micelles Studied by Spin-Probe Technique**

| | 5-DSA | | | 16-DSA | | |
|---|---|---|---|---|---|---|
| $T$ [K] | $\tau_R$ [$10^{-9}$ s] | $H(T)$ | $\eta$ [cP] | $\tau_R$ [$10^{-9}$ s] | $H(T)$ | $\eta$ [cP] |
| 277 | 5.20 | 0.31 | 46.33 | 2.36 | 0.49 | 21.01 |
| 287 | 3.57 | 0.51 | 32.94 | 1.73 | 0.49 | 15.96 |
| 297 | 2.66 | 0.51 | 25.45 | 0.96 | 0.49 | 9.13 |
| 307 | 1.80 | 0.51 | 17.80 | 0.64 | 0.49 | 6.31 |
| 317 | 1.43 | 0.51 | 14.60 | 0.45 | 0.56 | 4.56 |
| 327 | 1.04 | 0.51 | 10.94 | 0.32 | 0.56 | 3.35 |

The values of $H(T)$ for the micellar solutions of the $C_n(DAPANO)_2$ series were practically independent of the surfactant alkyl chain length (see Table 2), but were found to be slightly dependent on temperature (Table 3) and significantly on surfactant concentration (Table 2), varying from 1 for C/CMC = 0.3 to 0.58 for C/CMC = 100. It is known that $H(T)$ can be regarded as a rating of micelle solubilization properties and from its measured values it can be concluded that only the $C_n(DAPANO)_2$ concentration has a significant impact on the spin probe location in the micellar systems under investigation.

The spin probe technique enables one to determine not only micropolarity, but also the microviscosity ($\eta$) around the probe in micellar systems via the monitoring of $\tau_R$.[10c,12c,29,35] The microviscosity parameters of the studied systems were calculated from the Debye−Stokes−Einstein equation describing the direct relation between $\tau_R$ and $\eta$:

$$\tau_R = \frac{4\pi\eta R^3}{3kT} \quad (8)$$

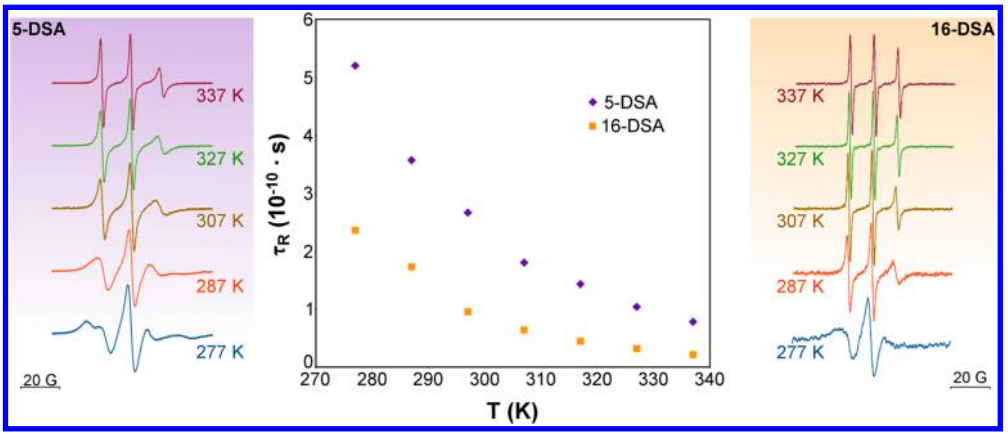


**Figure 4.** Variation of the rotational correlation time ($\tau_R$) of 5-DSA and 16-DSA in the water solutions of $C_{12}(DAPANO)_2$ (C/CMC concentration = 100) with temperature, in addition the exemplary EPR spectra are shown.


dx.doi.org/10.1021/jp306282m | J. Phys. Chem. B 2012, 116, 14324−14332

Table 4. Selected Properties of Examined Micellar Systems

| surfactant | DLS | | | DFT | | | | QSAR | |
|---|---|---|---|---|---|---|---|---|---|
| | PdI | $R_H^{DLS}$ [nm] | $V_{mic}^{DLS a}$ [nm$^3$] | $R_H^{DFT}$ [nm] | $V_{mon}^{DFT}$ [nm$^3$] | $V_{mic}^{DFT b}$ [nm$^3$] | $N_{agg}^{DFT}$ | CPP | Log $P$ |
| $C_{10}(DAPANO)_2$ | 0.192 | 1.75 | 22.45 | 1.64 | 0.558 | 18.49 | 33 | 0.17 | 7.73 |
| $C_{12}(DAPANO)_2$ | 0.215 | 2.04 | 35.56 | 1.96 | 0.604 | 31.61 | 52 | 0.14 | 8.52 |
| $C_{14}(DAPANO)_2$ | 0.136 | 2.28 | 49.65 | 2.14 | 0.658 | 40.98 | 62 | 0.11 | 9.31 |
| $C_{16}(DAPANO)_2$ | 0.213 | 2.39 | 57.19 | 2.47 | 0.695 | 62.97 | 91 | 0.10 | 10.10 |

$^a V_{mic}^{DLS} = {}^4/_3 \cdot \pi \cdot (R_H^{DLS})^3$ $^b V_{mic}^{DFT} = {}^4/_3 \cdot \pi \cdot (R_H^{DFT})^3$

where $R$ is the hydrodynamic radius of the probe, $k$ and $T$ represent the Boltzmann constant and temperature, respectively.

As 5-DSA and 16-DSA tend to be located in the hydrophilic part and the hydrophobic part of the formed micelles, the microviscosity of the two regions can be determined (see Table 3) also as a function of temperature. The microviscosity magnitudes for the hydrophobic (16-DSA) and hydrophilic (5-DSA) parts were found to decrease with rising temperature. Nevertheless, the $\eta$ values determined for the hydrophilic part of the micelles were always higher than those for the hydrophobic part. Importantly, the $\tau_R$−temperature diagrams are similar for the two spin probes (shown in Figure 4 for $C_{12}(DAPANO)_2$), proving that the formed micelles are spherical in shape, which is crucial for practical applications. A similar observation was made in the case of the other examined surfactants.

**3.5. Aggregation Properties Determined Using DLS, DFT and QSAR Methods.** All of the DFT and QSAR computations were performed for the nonionic form of the surfactants shown to be dominant by the potentiometry experiments. This assumption proved to be accurate as the micelle radii calculated by DFT were found to be in good agreement with the ones determined experimentally by DLS (Table 4).

The critical packing parameter (CPP) obtained from QSAR computations for the studied surfactants are listed in Table 4. CPP is well-known to be helpful in determining the type of structure of the formed aggregates.[36,37] In general, in water solutions such structures can include predominantly spherical micelles (CPP < ${}^1/_3$), linear cylindrical micelles (${}^1/_3$ < CPP < ${}^1/_2$) or lamellar structures (CPP ≈ 1).[37] Regardless of hydrophobic chain length, the CPP values are clearly less than ${}^1/_3$, indicating that the surfactants of the $C_n(DAPANO)_2$ series tend to form spherical micelles. This theoretical finding, in conjunction with the observed temperature variation of $\tau_R$ for both the spin probes (Figure 4), compellingly proves that micellar systems formed by the di-*N*-oxides under investigation are spherical in shape.

The approximate size of the micellar aggregates was estimated using the DLS method and the Stokes−Einstein equation. The polydispersity indexes (PdI), hydrodynamic radii ($R_H^{DLS}$) and micelle volumes ($V_{mic}^{DLS}$) for $C_n(DAPANO)_2$, along with their theoretically calculated counterparts ($R_H^{DFT}$, $V_{mic}^{DFT}$) and aggregation numbers ($N_{agg}^{DFT}$), are collected in Table 4. The studied di-*N*-oxides form small micelles whose hydrodynamic radii ($R_H^{DLS}$) increase with hydrophobic chain length from 1.75 for $C_{10}(DAPANO)_2$ to 2.39 nm for $C_{16}(DAPANO)_2$. Hence, the micelle radii can be directly controlled by the number of carbon atoms in the aliphatic chain. A similar phenomenon was observed, for instance, for the homologous series of fluorinated surfactants.[38] Although this rule seems to be taken for granted, several exceptions have been reported, for example, the tendency for micelle radii to increase with the number of carbon atoms in the aliphatic chain was not observed for fluorinated surfactants in ref 39. The polydispersity indexes (PdI) were found to be close to 0.2, indicating a monodispersive character of all the $C_n(DAPANO)_2$ surfactant solutions. This means that the surfactants under study form micelles of not only spherical in shape, but also similar in size, the properties of which are especially desirable in practical applications.

The aggregation numbers ($N_{agg}^{DFT}$) were determined by the DFT method, assuming a spherical shape (as proved by the EPR measurements and the QSAR calculations) of the micellar aggregates. Therefore, the first micelle volumes $V_{mic}^{DFT}$ were calculated from the equation:

$$V_{mic}^{DFT} = 4/3 \cdot \pi \cdot (R_H^{DFT})^3 \quad (9)$$

leading to the simple expression for $N_{agg}$:

$$N_{agg} = V_{mic}^{DFT}/V_{mon}^{DFT} \quad (10)$$

where $R_H^{DFT}$ and $V_{mon}^{DFT}$ (the volume of a monomeric surfactant molecule) are obtained directly from the DFT calculations. The $R_H^{DFT}$, $V_{mon}^{DFT}$, $V_{mic}^{DFT}$, and $N_{agg}$ values are listed in Table 4. A comparison of $R_H^{DFT}$ and $R_H^{DLS}$ shows very good agreement between the theory and the experiment. Moreover, all of the investigated surfactants had a very similar (almost planar) molecular structure. This means that a change in the length of the aliphatic chain has no major impact on the general structure of a monomeric surfactant molecule. The most important theoretically predicted feature, common for all the studied surfactants, is the asymmetric arrangement of the two heads (illustrated in Figure 5). Since the differences between the molecular structures are insubstantial, the calculated $R_H^{DFT}$, $V_{mon}^{DFT}$ and $V_{mic}^{DFT}$ values exclusively depend on the number of carbon atoms in the aliphatic chain. As a consequence, the $N_{agg}$ number is predicted to rise sharply when the chain is extended from 33 for $C_{10}(DAPANO)_2$ to 91 for $C_{16}(DAPANO)_2$. The increase in $N_{agg}$ with alkyl chain length is correlated with the decrease in the critical packing parameter (CPP). The $N_{agg}$ predicted for $C_n(DAPANO)_2$ can be compared with that of typical (single-head single-tail) *N*-oxide surfactants (*N*,*N*-dimethyldodecylamine oxides, DDAO). The $N_{agg}$ determined experimentally by Henmann et al. for nonionic DDAO micelles was found to amount to 76 in pure water.[40] This number is significantly higher than for the studied herein dicephalic di-*N*-oxide ($C_{12}(DAPANO)_2$) with the same chain length ($N_{agg}$ = 52). This is logical since single-chained surfactants with multiple head groups have a larger and more hydrophilic end in comparison with a single-head single-chain surfactant, which, as reported previously,[2a] results in several unique properties of their aggregate states, such as a lowered aggregate size and aggregation number.


dx.doi.org/10.1021/jp306282m | J. Phys. Chem. B 2012, 116, 14324−14332

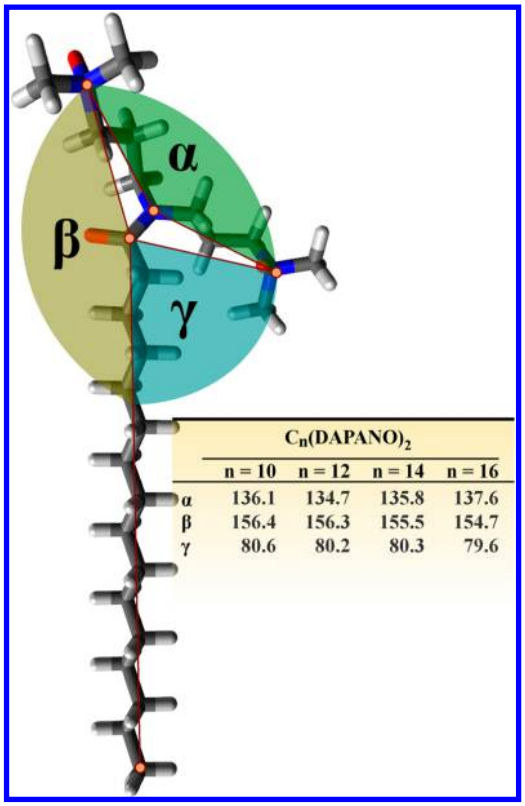


**Figure 5.** Asymmetric arrangement of two polar heads of the investigated surfactants; $\alpha$, $\beta$, $\gamma$ are given in degrees.

The hydrophobicity of the investigated surfactants can be illustrated with the values of log *P*, where *P* is the octanol–water partition coefficient for a given compound; log *P* is directly related to surfactant activity. As expected, the calculated values of log *P* increase with the length of the aliphatic chain. However, to put the logP values into perspective, it is sensible to compare them with those obtained for the $C_{12}(TAPAX)_2$ cationic analogue[1c] of $C_{12}(DAPANO)_2$. The log *P* value of 2.77 calculated by Skrzela et al. for $C_{12}(TAPAX)_2$ is significantly lower than 8.52 for $C_{12}(DAPANO)_2$. In addition, the $A_{min}$ (the minimum surface area demand per molecule) values measured for $C_{12}(DAPANO)_2$ are approximately 20% higher than for $C_{12}(TAPAX)_2$. The two facts clearly indicate higher surface activity of the reported nonionic surfactants.

## 4. CONCLUSIONS

The potentiometric titration experiments carried out on the *N*,*N*-bis[3,3′-(dimethylamine)propyl]alkylamide di-*N*-oxides have shown that at a pH close to physiological the $C_n(DAPANO)_2$ surfactants can be treated as nonionic. At the same time, the titrations have proven the di-*N*-oxides to be pH-sensitive in acidic environments. The surface tension measurements have shown that the interfacial behavior of the dicephalic surfactants depends on their specific molecular structure: the double-head surfactants exhibit lower surface activity in comparison with the monohead N-oxide surfactant, but significantly higher than their double-head cationic counterparts. The aggregation properties of micellar and premicellar solutions were studied by EPR using two nitroxide spin probes. The CMCs obtained from the experiments were in good agreement with those determined by surface tension measurements. In order to fully characterize the investigated micellar systems, their microviscosity and micropolarity were determined using the EPR technique. Also, changes in these properties as a function of temperature were examined. Dynamic light scattering and in silico methods (DFT and QSAR) were used to study the micellar properties of $C_n(DAPANO)_2$. The micelles derived from the surfactants under investigation were shown to be of spherical shape and of small size (with a low aggregation number). However, the size of the formed micellar systems was found to significantly increase with the length of the hydrophobic chain of the monomeric surfactant molecule. Moreover, the low polydispersity index values determined experimentally by DLS for the micellar solutions of $C_n(DAPANO)_2$ indicate that the formed micelles are remarkably homogeneous in size. For all of the investigated surfactants, changes in aliphatic chain length have been shown to have no major impact on the general structure of a monomeric surfactant molecule. The theoretically predicted asymmetric arrangement of the two head groups is a highly interesting feature of $C_n(DAPANO)_2$.

## AUTHOR INFORMATION

### Corresponding Author

*Phone: +48 71 3202828; fax: +48 71 3203678; e-mail: kazimiera.wilk@pwr.wroc.pl.

### Notes

The authors declare no competing financial interest.

## ACKNOWLEDGMENTS

This work was financed by a statutory activity subsidy from the Polish Ministry of Science and Higher Education for the Faculty of Chemistry of Wrocław University of Technology and for the Faculty of Chemistry of Wrocław University. All DFT calculations were performed using the computers of the Wrocław Center for Networking and Supercomputing (Grant No. 47).

## REFERENCES

(1) (a) Bazylińska, U.; Skrzela, R.; Szczepanowicz, K.; Warszyński, P.; Wilk, K. A. *Soft Matter* **2011**, *7*, 6113–6124. (b) Bazylińska, U.; Skrzela, R.; Piotrowski, M.; Szczepanowicz, K.; Warszyński, P.; Wilk, K. A. *Bioelectrochemistry* **2012**, *87*, 147–153. (c) Skrzela, R.; Para, G.; Warszyński, P.; Wilk, K. A. *J. Phys. Chem. B* **2010**, *114*, 10471–10480. (d) Frąckowiak, R.; Para, G.; Warszyński, P.; Wilk, K. A. *Colloids Surf. A* **2012**, *413*, 108–114. (e) Bazylińska, U.; Pietkiewicz, J.; Saczko, J.; Nattich-Rak, M.; Rossowska, J.; Garbiec, A.; Wilk, K. A. *Eur. J. Pharm. Sci.* **2012**, *47*, 406–420.

(2) (a) Bhattacharya, S.; Samanta, S. K. *J. Phys. Chem. Lett.* **2011**, *2*, 914–920. (b) Bhattacharya, S.; De, S. *Chem.—Eur. J.* **1999**, *5*, 2335–2347. (c) Ewert, K. K.; Evans, H. M.; Zidovska, A.; Bouxsein, N. F.; Ahmad, A.; Safinya, C. R. A. *J. Am. Chem. Soc.* **2006**, *128*, 3998–4006. (d) Jayaprakash, K. N.; Lu, J.; Fraser-Reid, B. *Angew. Chem., Int. Ed.* **2005**, *44*, 5894–5898.

(3) (a) Maeda, H. *Colloids Surf. A* **1996**, *109*, 263–271. (b) Goldsipe, A.; Blankschtein, D. *Langmuir* **2006**, *22*, 3547–3559.

(4) (a) Singh, S. K.; Bajpai, M.; Tyagi, V. K. *J. Oleo Sci.* **2006**, *55*, 99. (b) Garcìa, M. T.; Campos, E.; Ribosa, I. *Chemosphere* **2007**, *69*, 1574–1578.

(5) Niedziółka, K.; Szymula, M.; Lewińska, A.; Wilk, K. A.; Narkiewicz-Michałek J. *Colloids Surf. A* 2012, DOI: 10.1016/j.colsurfa.2012.02.047.

(6) (a) Sauer, J. D. *Amine Oxides* In *Cationic Surfactants: Organic Chemistry: (Surfactant Science Series)*; Richmond, J. M., Ed.; Marcel Dekker: New York, 1990; Vol. *34*. (b) Vaikunth, S. P. US Patent 5,866,718, 1999. (c) Karsa, D. R., Ed. *Industrial Applications of Surfactants*; Royal Chemical Society of Chemistry: Cambridge, UK,

1999. (d) Mel'nikova, Y. S.; Lindman, B. *Langmuir* **2000**, *16*, 5871−5878. (e) Goracci, L.; Germani, R.; Savelli, G.; Bassani, D. M. *ChemBioChem* **2005**, *6*, 197−203.
(7) (a) Gradzielski, M.; Hoffmann, H. *J. Phys. Chem.* **1994**, *98*, 2613. (b) Warisnoicharoen, W.; Lansley, A. B.; Lawrence, M. J. *Int. J. Pharm.* **2000**, *198*, 7−27.
(8) (a) Cross, J. Cationic Surfactants. In *Analytical and Biological Evaluation (Surfactant Science Series)*; Cross, J., Singer, J., Eds.; Marcel Dekker: New York, 1994; Vol. 53. (b) Domingo, X. *A Guide to the Surfactants World*; Proa.: Barcelona, Spain, 1995. (c) Ghosh, S.; Das Burman, A.; De, G. C.; Das, A. R. *J. Phys. Chem B* **2011**, *115*, 11098−11112.
(9) (a) Fukada, K.; Kawasaki, M.; Kato, T.; Maeda, H. *Langmuir* **2000**, *16*, 2495−2501. (b) Biondini, D.; Brinchi, L.; Germani, R.; Savelli, G. *Eur. J. Org. Chem.* **2005**, *14*, 3060−3063. (c) Mel'nikova, Y. S.; Lindman, B. *Langmuir* **2000**, *16*, 5861−5878. (d) Goracci, L.; Germani, R.; Savelli, G.; Bassani, D. M. *ChemBioChem* **2005**, *6*, 197−203. (e) Maeda, M.; Muroi, S.; Kakehashi, R. *J. Phys. Chem. B* **1997**, *101*, 7378−7382.
(10) (a) Dragutan, I.; Dragutan, V.; Caragheorgheopol, A.; Zarkadis, A. K.; Fischer, H.; Hoffmann, H. *Colloids Surf. A* **2001**, *183−185*, 767−776. (b) Caldararu, H. *Spectrochim. Acta A* **1998**, *54*, 2309−2336. (c) Wilk, K. A.; Zielińska, K.; Hamerska-Dudra, A.; Jezierski, A. *J. Colloid Interface Sci.* **2009**, *334*, 87−95.
(11) Vasilescu, M.; Caragheorgheopol, A.; Caldararu, H. *Adv. Colloid Interface Sci.* **2001**, *89−90*, 169−194.
(12) (a) McCarney, E. R.; Armstrong, B. R.; Kausik, R.; Han, S. *Langmuir* **2008**, *24*, 10062−10072. (b) Lebedeva, N.; Bales, B. L. *J. Phys. Chem. B* **2006**, *110*, 9791−9799. (c) Zielińska, K.; Wilk, K. A.; Jezierski, A.; Jesionowski, T. J. *Colloid Interface Sci.* **2008**, *321*, 408−417.
(13) Skrzela, R.; Piasecki, A.; Wilk, K. A. *Novel surface active di-N-oxides of 3,3′-iminobis(N,N-dimethylpropylamine) and method of their production*, patent application P387268 (2009).
(14) (a) Gans, P.; Sabatini, A; Vacca, A. *J. Chem. Soc., Dalton Trans.* **1985**, 1195−1200. (b) Gans, P.; Sabatini, A.; Vacca, A. *Talanta* **1996**, *43*, 1739−1753.
(15) Bales, B. L.; Ranganathan, R.; Griffiths, P. C. *J. Phys. Chem. B* **2001**, *105*, 7465−7473.
(16) Frisch, M. J.; et al. Gaussian 09, Revision A.2; Gaussian, Inc.: Wallingford. CT, 2009.
(17) (a) Yanai, T.; Tew, D. P.; Handy, N. C. *Chem. Phys. Lett.* **2004**, *393*, 51−57. (b) Lee, C. T.; Yang, W. T.; Parr, R. G. *Phys. Rev. B* **1988**, *37*, 785−789. (c) Becke, A. D. *J. Chem. Phys.* **1993**, *98*, 5648−5652. (d) Stephens, P. J.; Devlin, F. J.; Chabalowski, C. F.; Frisch, M. J. *J. Phys. Chem.* **1994**, *98*, 11623−11627.
(18) (a) Hariharan, P. C.; Pople, J. A. *Theor. Chim. Acta* **1973**, *28*, 213−222. (b) Clark, T; Chandrasekhar, J.; Schleyer, P. *J. Comput. Chem.* **1983**, *4*, 294−301.
(19) (a) Cancès, E.; Mennucci, B.; Tomasi, J. *J. Chem. Phys.* **1997**, *107*, 3032−3041. (b) Tomasi, J; Mennucci, B.; Cancès, E. *J. Mol. Struct. (Theochem)* **1999**, *464*, 211−226. (c) Tomasi, J.; Mennucci, B.; Cammi, R. *Chem. Rev.* **2005**, *105*, 2999−3093.
(20) (a) Ferreira, T. L.; Sato, B. M.; El Seoud, O. A.; Bertotti, M. *J. Phys. Chem. B* **2010**, *114*, 857−862. (b) Neese, F. *Coord. Chem. Rev.* **2009**, *253*, 526−563. (c) Witwicki, M.; Jerzykiewicz, M.; Jaszewski, A. R.; Jezierska, J.; Ozarowski, A. *J. Phys. Chem. A* **2009**, *113*, 14115−14122. (d) Witwicki, M.; Jezierska, J. *J. Phys. Chem. B* **2011**, *115*, 3172−3184.
(21) Hansch, C.; Maloney, P. P.; Fujita, T.; Muir, R. M. *Nature* **1962**, *194*, 178.
(22) (a) Martins, J. P. A.; Barbosa, E. G.; Pasqualoto, K. F. M.; Ferreira, M. M. C. *J. Comput.-Aided. Mol. Des.* **1988**, *2*, 145. (b) Puzyn, T., Leszczynski, J., Cronin, M. T., Eds. *Challenges and Advances in Computational Chemistry and Physics, Vol. 8: Recent Advances in QSAR Studies*; Springer: Dordrech, Germany, 2010.
(23) *HyperChem, version 8.0*; HyperCube Inc.: Gainesville, FL.
(24) (a) Viswanadhan, V. N.; Ghose, A. K.; Revankar, G. N.; Robins, R. K. *J. Inf. Comput. Sci.* **1989**, *29*, 163. (b) Ghose, A. K.; Pritchett, A.; Crippen, G. M. *J. Comput. Chem.* **1988**, *9*, 80−90.
(25) (a) Piasecki, A; Piłakowska-Pietras, D; Baran, A.; Krasowska, A. *J. Surfact. Deterg.* **2008**, *11*, 187−194. (b) Piasecki, A.; Wójcik, B.; Łuczyński, J; Piłakowska-Pietras, D.; Witek, S.; Krasowska, A. *J. Surfact. Deterg.* **2009**, *12*, 201−207.
(26) (a) Rosen, J. M. *Surfactants and Interfacial Phenomena*, 3rd ed.; Wiley Interscience: New York, 2004. (b) Myers, D. *Surfactant Science and Technology*, 3rd ed.; John Wiley and Sons, Inc.: Hoboken, NJ, 2006. (c) Florence, A. T.; Attwood, D. *Physicochemical Principles of Pharmacy*, 5th ed.; TJ International: Padstow, Cornwall, UK, 2011.
(27) Likhtenshtein, G. I.; Yamauchi, J.; Nakatuji, S.; Smirnov, A.; Tamura, R. *Nitroxides: Application in Chemistry, Biomedicine, and Materials Science*; WILEY-VCH: Weinhem, Germany, 2008.
(28) Stone, T. J.; Buckman, T.; Nordio, P. L.; McConnell, H. M. *Proc. Natl. Acad. U.S.A.* **1965**, *54*, 1010−1016.
(29) Wilk, K. A.; Zielińska, K.; Jezierski, A. *Colloids Surf. A* **2009**, *343*, 64−69.
(30) Zoumpanioti, M.; Stamatis, H.; Papadimitriou, V.; Xenakis, A. *Colloids Surf. B* **2006**, *47*, 1−9.
(31) Bahri, M. A.; Hoebeke, M.; Grammenos, A.; Delanaye, L.; Vandewalle, N.; Seret, A. *Colloids Surf. A* **2006**, *290*, 206−212.
(32) Cohen, A. H.; Hoffman, B. M. *Inorg. Chem.* **1974**, *13*, 1484−1491.
(33) (a) Bales, B. L.; Shahin, A.; Lindblad, C.; Almgren, M. *J. Phys. Chem. B.* **2000**, *104*, 256−263. (b) Lewińska, A.; Wilk, A. K.; Jezierski, A. *J. Sol. Chem.* **2012**, *41*, 1210−1223.
(34) Bales, B. L.; Ranganathan, R.; Griffiths, P. C. *J. Phys. Chem. B.* **2001**, *105*, 7465−7473.
(35) Lebedeva, N.; Ranganathan, R.; Bales, B. L. *J. Phys. Chem. B* **2007**, *111*, 5781−5793.
(36) Li, D.; Wu, H.; Li, Z.; Cong, X.; Sun, J.; Ren, Z.; Liu, L.; Li, Y.; Fan, D.; Hao, J. *Colloids Surf. A* **2006**, *274*, 18.
(37) Israelachvili, J.; Ladyzhinski, I. The Physico-Chemical Basis of Self-Assembling Structures. In *Forces, Growth and Form in Soft Condensed Matter: At the Interface between Physics and Biology*;Skjeltorp, A. T., Belushkin, A. V., Eds.; Kluwer Academic Publisher: Netherlands, 2005.
(38) (a) Matsuoka, K.; Yonekawa, A.; Ishii, M.; Honda, C.; Endo, K.; Moroi, Y.; Abe, Y.; Tamura, T. *Colloid Polym. Sci.* **2006**, *285*, 323−330. (b) Matsuoka, K.; Yoshimura, T.; Shikimoto, T.; Hamada, J.; Yamawaki, M.; Honda, C.; Endo, K. *Langmuir* **2007**, *23*, 10990−10994.
(39) Matsuoka, K.; Chiba, N.; Tomokazu, Y.; Takeuchi, E. *J. Colloid Interface Sci.* **2011**, *356*, 624−629.
(40) Henmann, K. W. *J. Phys. Chem.* **1962**, *66*, 295−300.